D15:
Simulation of a Dust Event over Cyprus

An episode of low visibility was observed over Cyprus in late September 2011. It appears that it was caused by an increase in the atmospheric dust concentration near the surface. This episode is selected in order to present and check the chemical model performance used within AIRSPACE project. A high-resolution atmospheric chemistry general circulation model (AC-GCM) was used to simulate the emissions, transport and deposition of airborne desert dust. The model configuration used involves the spectral resolution T255L31 (0.5°, 50Km) and 31 vertical levels in the troposphere and lower stratosphere. The model reproduces the dust distribution and timing, in good agreement with observations, which is illustrated by MODIS satellite images. Our preliminary analysis shows that the increase in the aerosol concentration resulted from the mineral dust transport primarily from the Negev desert, which was deposited over Cyprus. In addition, a minor dust event from the Sahara occurred in this period, but the particles were removed from the atmosphere by precipitation before the plume reached Cyprus.

Introduction

An episode of low visibility was observed over the Eastern Mediterranean (EM) and particularly over Cyprus in September 2011 as a result of a dust storm. Figure 1 shows a MODIS satellite image over the EM and the dust storm over Cyprus. As suggested by the aerosol optical depth (AOD) gradient in the figure, the dust was emitted from the southern Negev desert on 27th of September. By the 28th of September, the dust deposited over Cyprus.

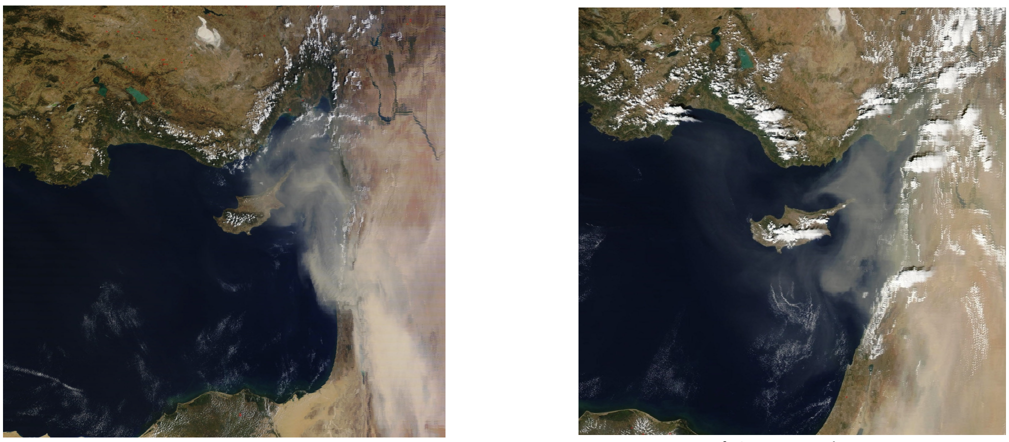

27th of September 2011   28th of September 2011

Figure 1: NASA MODIS satellite images showing the dust storm that reached Cyprus

Model Description

A high resolution atmospheric Chemistry General Circulation Model (AC-GCM) is used to study the emission, transport and deposition of dust in the referenced period. The Modular Earth Sub-model System (MESSy version 2.41) [4, 5, 6] is an earth system model, which is capable of running with multiple representations of processes simultaneously coupled to the core atmospheric general circulation model (ECHAM5). The model configuration used in the present study has a spectral resolution of T255L31 (0.5°, 50Km) and 31 vertical levels up to 10 hPa. Reference [3] emphasizes the importance of higher resolution simulations for better dust representation in the model. The model output is averaged and stored over 5hr intervals, which provides an entire diurnal cycle after 5 days. The configuration also includes a simplified sulphate chemistry scheme [3] allowing the production of sulphuric acid and particulate sulphate, which play an important role in transforming the dust particles from hydrophobic into hydrophilic, thus affecting their ability to interact with clouds and be removed by precipitation [1]. The ammonia (NH_3) reaction with sulphate and corresponding coating with dust [2] is also considered in this study. Since we concentrate on dust episodes we applied a reduced version of the atmospheric chemistry scheme, which does not account for secondary inorganic and organic aerosol species associated with air pollution. The model was nudged towards ERA40 reanalysis data to represent the actual meteorological conditions, according to a Newtonian relaxation data assimilation method [1]. The model simulation was performed over the period September-October 2011 (with 15 days spin up time). In the following we largely concentrate on a period of reduced visibility in Cyprus in late September.

Model Evaluation

The model results were evaluated using the AOD provided by the NASA AErosol RObotic NETwork (AERONET) available from http://aeronet.gsfc.nasa.gov. The data comparison represents the AOD for all aerosols simulated in the model as well as observed in the atmosphere at 550nm wavelength. The observed AOD was averaged over the 5hr output intervals as well as the averaged AOD over the same period from the model. Figure 2 shows the eight AERONET stations from which observational data were available during the simulation period and were used in this study. These stations are not necessarily located in dust-dominated regions but can be more strongly affected by other aerosol types, including air pollution.

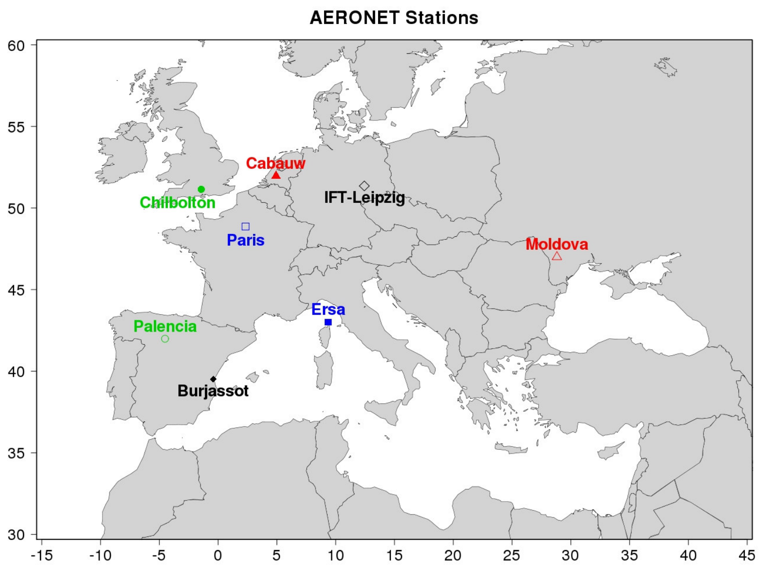

Figure 2. AERONET stations used to evaluate the model results

The scatter plot between the modeled and observed AOD is shown in figure 3. Different colors and symbols are used for each station ID (see legend). As shown in the figure, the model is capable of simulating the AOD in general. However, at some stations (Leipzig, Palencia, Paris) the model tends to underestimate the observed AOD. This is explained by the use of the reduced atmospheric chemistry scheme in the model that does not fully account for urban air pollution in addition to the unresolved physics at small scales in the global models.
Figure 4 shows the time evolution of the AOD for different stations. As shown in the figure, the model is capable of simulating the AOD for all stations.

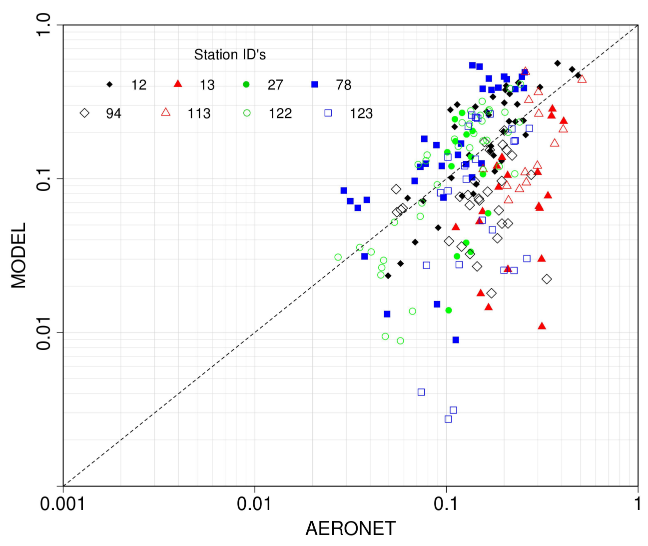

Figure 3. Scatter plot between modeled and observed AOD for different AERONET stations

As shown in figure 4a, the model is performing well at this station besides an overestimation in the period between 22-26th of September. This disagreement may result from local conditions that are not resolved by the model at this resolution. A similar tendency was also noticed at station Ersa (Figure 4d). The model underestimates AOD over the stations Cabauw and Moldova (Figure 4b and f). For the rest of the stations the model is in a very good agreement with observations in both magnitude and timing. In summary, the comparison between the modeled and observed AOD indicates the ability of the model to simulate the AOD rather well.

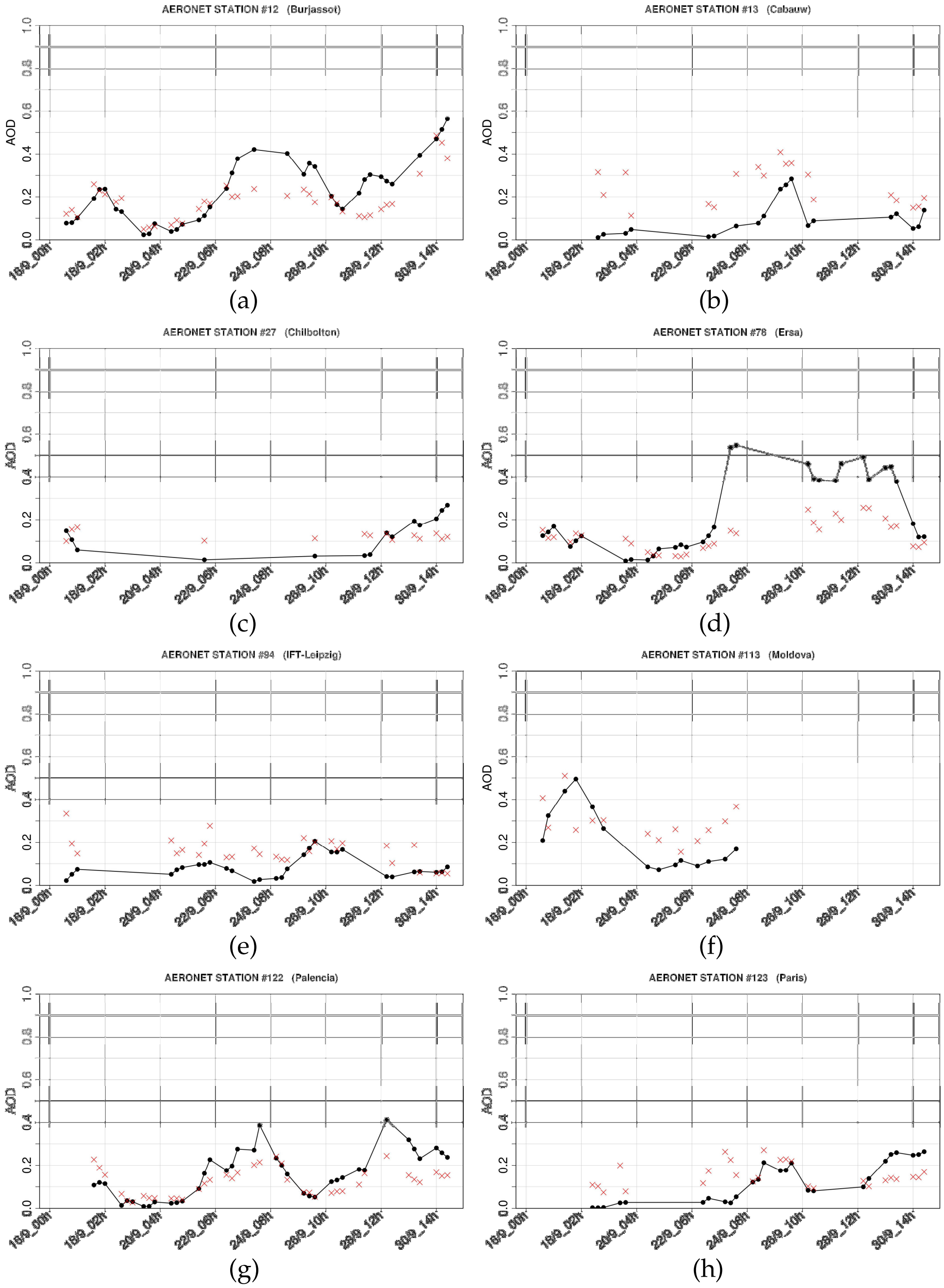

Figure 4. Comparison between the modeled (black) and observed (red) AOD for different stations

Dust Episode Assessment

Figure 5 depicts the daily average dust load over the EM region. As shown in the figure, the main dust source at that time is located in the north of Saudi Arabia and particularly the Negev desert, as well as some dust from sources in the eastern Sinai in Egypt. As a result of the strong surface wind during this period, the dust was emitted from these regions and transferred to the EM in the following days. The figure shows the velocity vectors as well as the stream lines at about 1.5km altitude (~850hPa). As shown in Figure 5c the dust reached Cyprus with the highest concentration on the 28th of September. By the 29th of September, the dust was removed from the atmosphere by different mechanisms. Figure 6 illustrates that the dust was transported from the source region to the EM at an elevation about 2500m above sea level (ASL). Comparing Figure 1 and Figure 5, the model is generally capable of simulating the dust emission, transport and deposition. Below we present some more details about the model simulation and the processes that caused the dust episode.

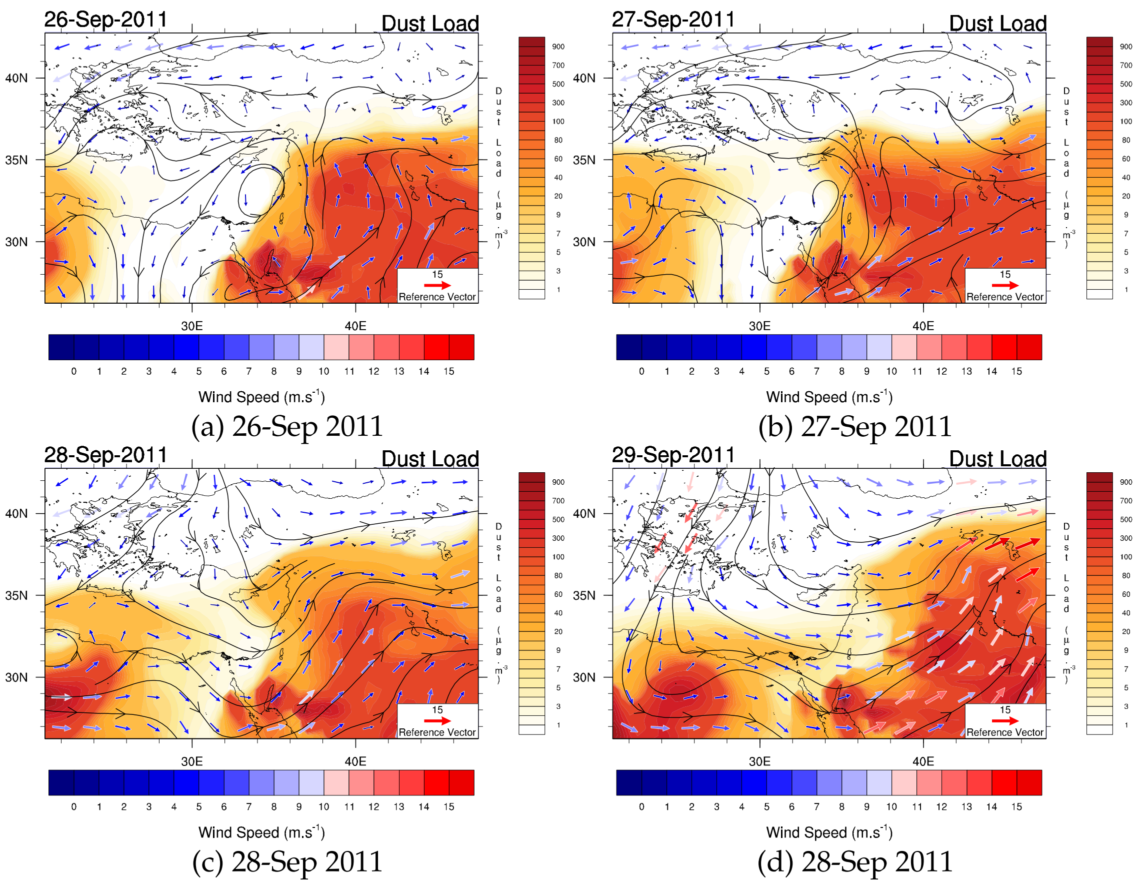

(a) 26-Sep 2011 (b) 27-Sep 2011

(c) 28-Sep 2011 (d) 28-Sep 2011

Figure 5. Daily average of dust load over the Eastern Mediterranean

A latitudinal cross section at 35.5˚N is presented in Figure 6. The dust was transported over the EM to Cyprus on the 26th and 27th of September. As shown in Figure 6b, the dust was elevated from the Negev desert around 45˚E and then transported over the high-pressure cell around 43˚E. At the source region, the dust concentration reached 100μg.m^{-3}. On the next day, (Figure 6), the dust reached Cyprus and the surface concentration was 8μg.m^{-3} with the highest concentration of 100μg.m^{-3} obtained at 2500m ASL and 40˚E as shown in Figure 6 c. By the 29th of September, the dust was removed from the atmosphere over Cyprus and the concentration was significantly decreased over the island to less than 1μg.m^{-3} and the high pressure cell was broken up. The high pressure system over the EM was associated with stable atmospheric conditions, maintaining the elevated transport at 2500m ASL as shown in Figure 6b. In addition, a small amount of dust was transported from the Sahara to the EM but according to our model results it did not reach Cyprus. The main dust contribution during this period originated from the Negev and the northern Saudi Arabian deserts.

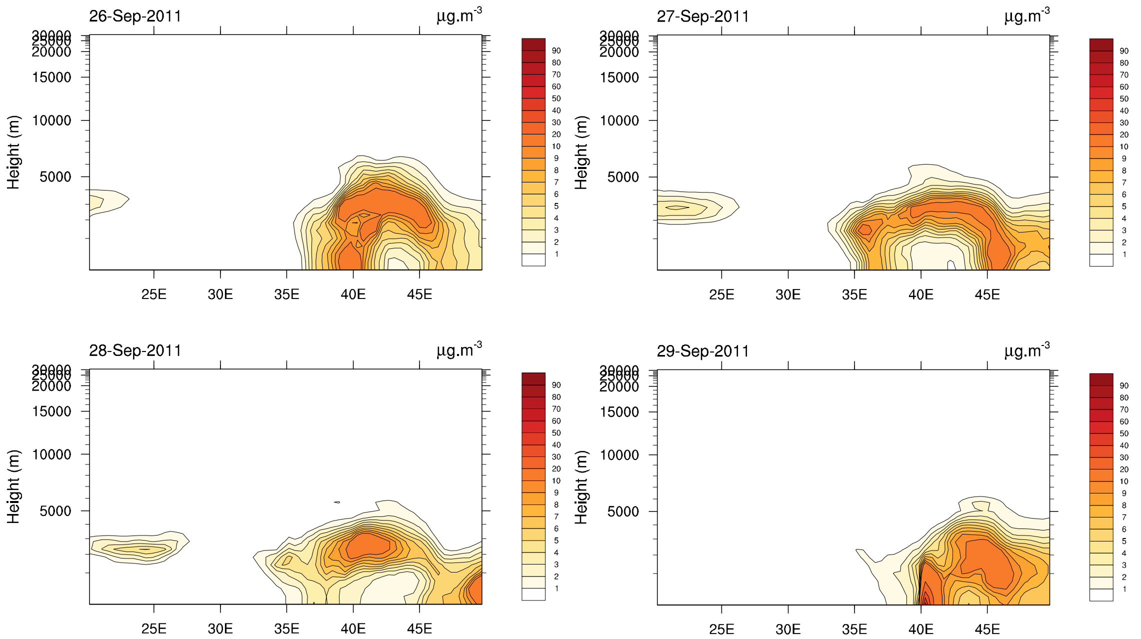

Figure 6. Latitude cross section of daily average of dust at 35.5N

Figure 7 shows the time history at Agia-Marina station (33.0583˚E, 35.0355˚N) for different aerosol and gas concentrations (μg.m^{-3}) simulated by the model at two heights; a) 2500m and b) the surface. The 2500m elevation was selected related to the dust transport elevation as shown in Figure 6. Figure 7 shows the diurnal cycle for different species including Sulphuric Acid, Nitrate Monoxide and Sulphur Dioxide. The diurnal cycle for many compounds results from the photolysis reactions in the model [3]. As shown in Figure 7, the dust concentration for all modes (soluble and insoluble) was almost constant before the 21st of September at the surface level, which corresponds to the background dust level in this area. As presented in the same figure, the soluble mode of dust is one order of magnitude higher than the insoluble part. This resulted from the coating of the dust particles by anthropogenic sulphur compounds. On the 22nd of September, the aerosol concentration was increased due to a dust event coming from the Sahara, which lasted for a few hours. However, this event had only a minor contribution. On the 25th of September, dust was transported (insoluble) resulting in an increased concentration at the surface that lasted for four days and caused limited visibility conditions. On the 28th of

September, the coarse and accumulation modes (DU_ci, Du_ai) were enhanced significantly and the total dust concentration was increased from 9×10^{-3} µg.m^{-3} to 7×10^{-1} µg.m^{-3}. At 2500 elevation, the DU_ci and DU_ai declined and resulted in a decrease in the total dust concentration from 10^{-1} µg.m^{-3} to 2×10^{-2} µg.m^{-3} due to the deposition of the dust from higher elevation to the surface. Afterwards, the total dust concentration was decreased at the surface due to deposition. By the 30th of September, the total dust concentration at the surface was decreased significantly to 8×10^{-1} µg.m^{-3} to 10^{-2} µg.m^{-3}. The increase in the total dust concentration at the surface resulted from the deposition from higher elevation, which was transported from remote areas (insoluble mode).

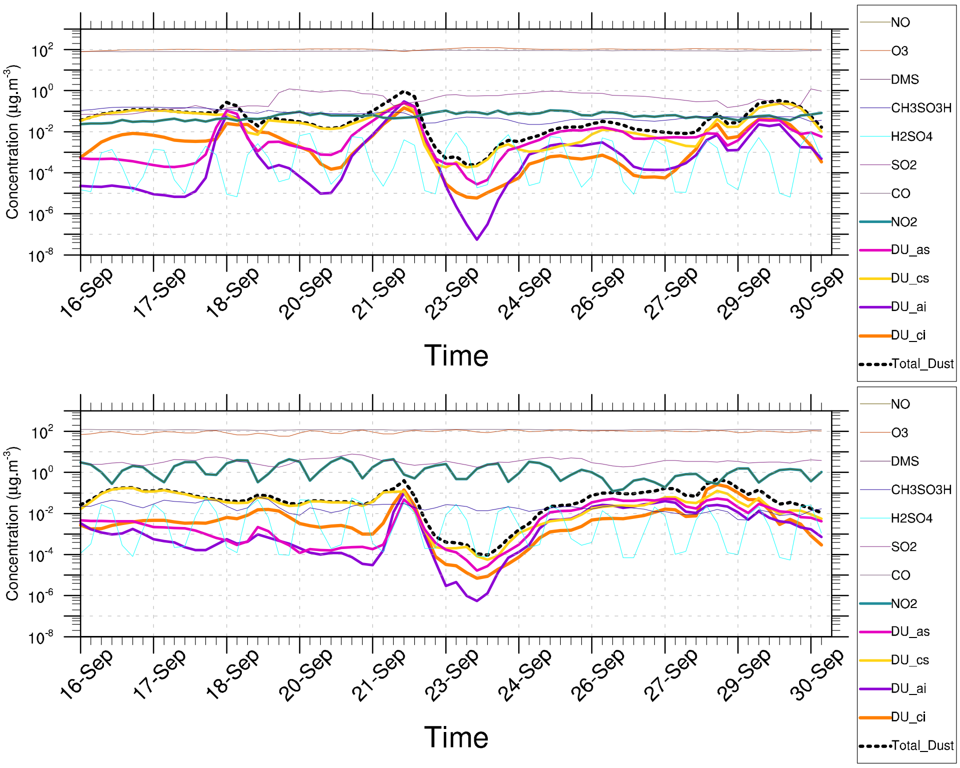

Figure 7. Time history for different species for 2500m elevation (upper panel) and surface (lower panel) at the Agia Marina station

Figure 8 shows the time evolution of the dust removal by wet and dry mechanisms as well as the total dust removal at the surface. As shown in the figure, starting from 20th of September, the dust was removed mainly by wet removal mechanism associated with precipitation. The blue contours show the TRMM precipitation satellite observations. The precipitation events started from the 20th of September from 20˚E longitude up to 40˚E. The figure shows that the wet dust removal, generally, coincides with the precipitation observations; however the model tends to overestimate the precipitation events. This resulted in too strong wet removal of the dust by the model. Subsequently, the dry removal was insignificant. This is also shown in Figure 7a at 2500m ASL illustrating the decrease in the dust concentration caused by precipitation. On the 23rd of September, the dry removal was significantly increased and dominated over the area from 35˚E to 50˚E and resulted in significant decreases of the dust on the 21st of September at the surface and 2500m ASL as shown in Figure 7. In addition, on the 27th of September, the dry removal increased again over the same area as well as the wet removal. Figure 7c shows the total dust removal from the atmosphere for both wet and dry mechanisms for the two modes. The dust was mainly removed from the atmosphere over the region of interest starting from 26th of September resulting in increased dust levels at the surface as shown in Figure 7b.

The increase in the total dust concentration at the surface resulted from the deposition from higher elevation, which was transported from remote areas.

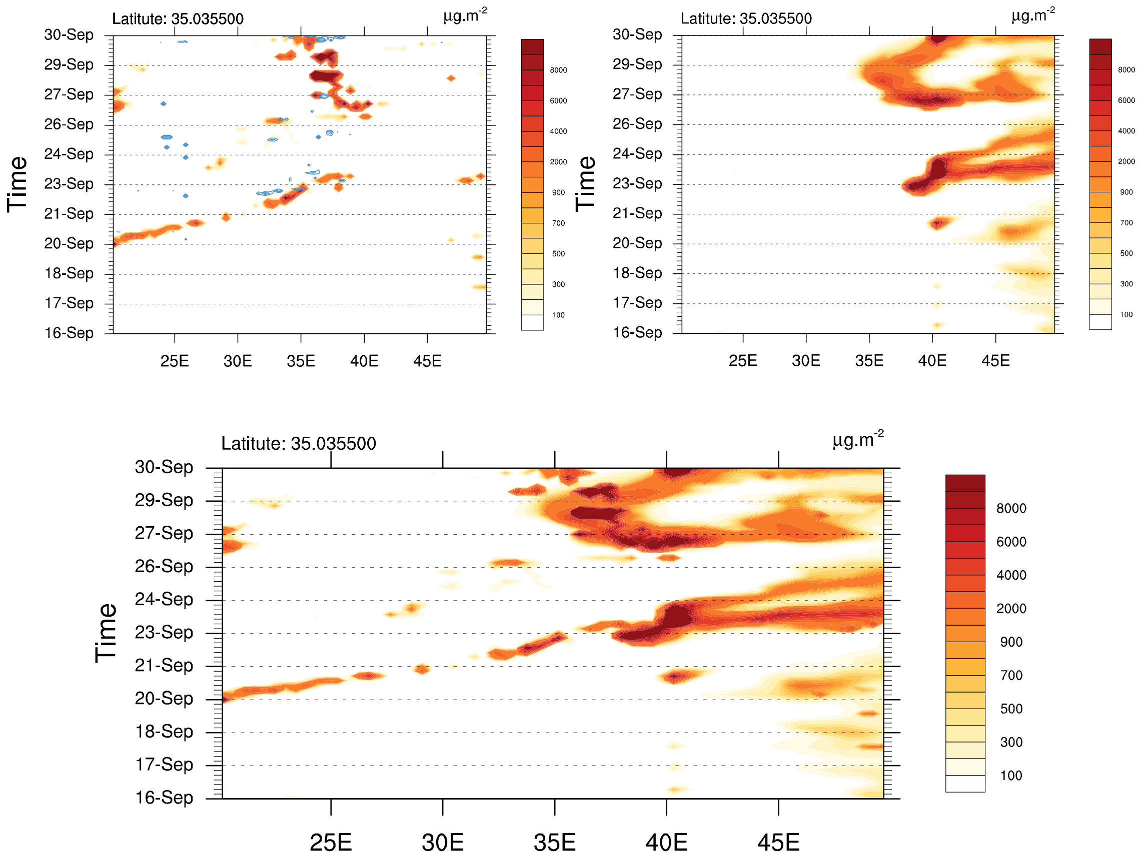

Figure 8. Time evolution of the dust removal at 35.5N at the surface

Conclusions

A dust storm episode was successfully modeled using a high-resolution version of the EMAC model at T255 spectral resolution and 31 vertical levels. The model simulates the simple sulphur chemistry mechanisms to simulate the transformation of the dust particles from the insoluble to soluble mode. The aerosol optical depth was evaluated using observed AOD from the AERONET stations and the model successfully reproduced the optical properties for the aerosols taken into account at this model resolution. The dust emissions were calculated online at each model time step as well as the aerosols microphysics using the GMXe sub-model. The model produced the dust distribution similarly to the observations presented in MODIS satellite images. The dust episode over Cyprus was analyzed and it appears that the event resulted from the transport of dust from the Negev desert to the Eastern Mediterranean with peak concentrations at 2500m elevation. The increase in the dust concentration at the surface resulted mainly from dry deposition over Cyprus starting from 26th to 30th of September Additional dust concentrations, transported from the Sahara, were simulated by the model on the 21st of September but lasted for a few hours only as the particles were efficiently removed by precipitation. Afterwards, the dust concentration was increased again over four days due to transport from the Negev desert and was subsequently removed by dry deposition. The observed lower visibility over Cyprus resulted from the sedimentation of the dust followed by dry deposition at the surface. The main contribution was from both pristine and coated dust particles during the episode. Before the episode, background coated dust (i.e., mixed composition) particles were dominated and the concentration was almost constant at the surface.

References

1. M. Astitha, J. Lelieveld, M. Abdel Kader, A. Pozzer, and A. de Meij. "New parameterization of dust emissions in the global atmospheric chemistry-climate model EMAC", Atmospheric Chemistry and Physics Discussions, 12(5):13237{13298, May 2012.
2. P. Ginoux, L. Clarisse, C. Clerbaux, P.-F. Coheur, O. Dubovik, N. C. Hsu, and M. Van Damme. Mixing of dust and NH3 observed globally over anthropogenic dust sources. Atmospheric Chemistry and Physics, 12(16):7351{7363, Aug. 2012.
3. G. Gleser, A. Kerkweg, and H. Wernli, "The mineral dust cycle in EMAC 2.40: sensitivity to the spectral resolution and the dust emission scheme". Atmospheric Chemistry and Physics, 12(3):1611{1627, Feb. 2012.
4. P. Joeckel, A. Kerkweg, A. Pozzer, R. Sander, H. Tost, H. Riede, A. Baumgaertner, S. Gromov, and B. Kern, "Development cycle 2 of the modular earth submodel system (MESSy2)", Geoscience Model Development, 3(2):717{752, Dec. 2010.
5. P. Joeckel, R. Sander, A. Kerkweg, H. Tost, and J. Lelieveld, "Technical note: The modular earth submodel system (MESSy) - a new approach towards earth system modeling", Atmospheric Chemistry and Physics, 5(2):433{444, Feb. 2005.
6. P. Joeckel, H. Tost, A. Pozzer, C. Bruehl, J. Buchholz, L. Ganzeveld, P. Hoor, A. Kerkweg, M. Lawrence, R. Sander, B. Steil, G. Stiller, M. Tanarhte, D. Taraborrelli, J. van Aardenne, and J. Lelieveld, "The atmospheric chemistry general circulation model ECHAM5/MESSy1: consistent simulation of ozone from the surface to the mesosphere", Atmospheric Chemistry and Physics, 6(12):5067{5104, Nov. 2006.
7. K. J. Pringle, H. Tost, S. Metzger, B. Steil, D. Giannadaki, A. Nenes, C. Fountoukis, P. Stier, E. Vignati, and J. Lelieveld, "Description and evaluation of GMXe: a new aerosol submodel for global simulations (v1)", Geoscience Model Development, 3(2):391{412, Sept. 2010.

D17: Chemical model disadvantages and the projection trends

Operational Strategy

The model utilized was the ECHAM5 (Max Plank Institute, http://www.mpimet.mpg.de/en/wissenschaft/modelle/echam/echam5.html) in 50km resolution. This is a global model therefor no boundary xconditions are necessary to be introduced to the model. All known emission sources are incuded while the initial conditions come from the ERA40 reanalysis data (ECMWF) at .5 degrees resolution. Every 12 hours of operation, the model fields are nudged towards the ERA40 data in order to simulate the meteorological conditions as precise as possible. In order to reduce the computational time the model uses a simplified chemistry module, preserving only the sulfate and NOx interactions which are considered the most important as far as the aerosols are considered.

To ensure that the model holds an adequate representation of the pollutants and the dust in the atmosphere, the model is running for 15 days (spin-off) to create from the Meteorology and the emissions the current weather conditions. This strategy ensures that the existed pollutants not represented in the model are removed from the atmosphere while the sources will produce pollutants that will be dispersed in the atmosphere. After the initial spin-off the atmospheric conditions represented from the model fields and the pollutant concentrations are considered as close to reality as possible. The comparison of the output of the model for the AOT with the measured values from the AERONET network indicates that the simulated atmosphere is close to reality concerning areas with similar climatological and industrial characteristics with Cyprus while for areas with heavy industry there is a significant deviation which can be justified from the reduced chemistry module used for the runs.

Identified issues for the operational run of the numerical model

The most significant issue for the operational run of a numerical model prediction of the dust is the complete absence of initial conditions for pollutant and dust concentrations This enforces the utilization of global models to simulate the atmosphere with extremely accurate emission inventories which are absent or not complete for north Africa and eastern Mediterranean. The latter is an important source of ambiguity for concentrations.

Furthermore, the sparse coverage of measurements for the spatial validation of the model in our region does not give us a clear picture for the evaluation assessment of the model.

The incumbent use of a global model enforces the utilization of a large grid due to computational limitations. The global grid introduces an adequate representation of the topography of the models and requires special parameterization of processes that often lead to errors.

Another issue is the simplified chemistry used for the simulation. The computational power that is necessary for the implementation of a full chemistry scheme is simply not available.